Journal of Alloys and Compounds, 187 (1992) 31–37
JALCOM 307

A structural irregularity of the stacking sequence in the $Sr_3V_2O_7$ compound

Shiro Takeno, Shin-ichi Nakamura, Noburu Fukushima and Ken Ando
Research and Development Center, Toshiba Corporation, Saiwai-ku, Kawasaki 210 (Japan)

(Received January 27, 1992)

Abstract

The presence of intergrowths in the $Sr_3V_2O_7$ compound has been elucidated by means of high resolution transmission electron microscopy and several types of atomic stacking sequence of the intergrowths, *i.e.* a stacking irregularity along the *c* direction of $Sr_3V_2O_7$, have been clarified. The intergrowths were composed of the $Sr_4V_3O_{10}$ phase, *i.e.* one of the related compounds $Sr_{n+1}V_nO_{3n+1}$. The presence of such intergrowths are considered to be produced by matrix compositional fluctuations.

1. Introduction

Since the discovery of high T_c superconducting ceramics [1–4], many related perovskite layered compounds have aroused great interest, and their physical properties have been gradually elucidated by many researchers. Recently, new layered perovskite compounds $Sr_{n+1}V_nO_{3n+1}$ have been synthesized, and their crystal structures have also been determined by means of X-ray or neutron diffraction techniques, and they can also be considered as polytypoids [5–8]. It is expected that these $Sr_{n+1}V_nO_{3n+1}$ compounds are constructed from double two-dimensional Sr–O layers and perovskite subcells and that the number of perovskite subcells increase in their unit cells as the value of n increases.

In the case of a bismuth-based superconducting system, the value of the critical transition temperature T_c is influenced by the number of two-dimensional Cu–O layers per unit cell, *i.e.* the variation on the *c* unit length [9, 10]. This is a typical example where a microscopic structure of a material influences its physical properties, and therefore it is very important to reveal such a microstructure. Now, it is expected that the above-mentioned $Sr_{n+1}V_nO_{3n+1}$ compounds will be candidates for new high T_c materials with appropriate doping [11]. However, there is very little information about their microstructural features such as stacking defects or intergrowths which are expected to be introduced into the $Sr_{n+1}V_nO_{3n+1}$ compounds [8], as shown in the bismuth-based superconducting system [10, 12–17]. In this study, the so-called intergrowths have been determined and their structural models have also been proposed.

0925-8388/92/$5.00

2. Experimental details

The $Sr_3V_2O_7$ sample was prepared by the following synthesis procedure: starting materials, $SrCO_3$ and V_2O_3; sintering temperature, 1273 K; sintering time, 10 h; atmosphere for synthesis, H_2 gas (with a 213 K dew point).

High resolution electron microscopy (HREM) and electron diffraction studies were carried out by the following procedure. First, the crystal was crushed into a very fine powder, and then the powder was widely dispersed on an amorphous carbon thin film with many holes [8]. We made [100]-zone HREM observations using a JEOL JEM-4000FX type transmission electron microscope at an accelerating voltage of 400 kV. Selected-area diffraction patterns of this compound were also obtained for structural analysis.

3. Results and discussion

Figure 1(a) shows a typical high resolution image taken with a beam incidence along the [100] direction of the $Sr_3V_2O_7$ crystal. Nozaki *et al.* [6] reported that $Sr_3V_2O_7$ has a tetragonal crystal structure and its lattice parameters are approximately $a = 0.38$ nm and $c = 2.03$ nm [6]: it is intuitively interpreted that the $Sr_3V_2O_7$ phase is dominant in Fig. 1(a). The multiple-beam lattice image in Fig. 1(a) is considered to have been obtained nearly under the so-called Scherzer condition, *i.e.* the projected cationic columns appear as black dots and the lighter cationic atoms often have a fainter black contrast in a very thin region [18]. It is known that $Sr_3V_2O_7$ has two types of (001)#plane, *i.e.* V–O planes and Sr–O planes, and they show a perovskite-like configuration. Therefore it is expected that the strontium atomic columns along the incident beam direction have a strong black contrast on a white background, and the relatively fainter black dots could be associated with the V–O atomic columns along the [100] direction. According to this rule, the double Sr–O planes along the [010] direction are indicated by small arrows at the edge of the sample in Fig. 1(a). Furthermore, intergrowths are clearly observed in the local regions and the phase of such intergrowths can be denoted as $Sr_4V_3O_{10}$, *i.e.* the $n = 3$ case for $Sr_{n+1}V_nO_{3n+1}$, since the measured distance between the double Sr–O layers is in good agreement with that for the $n = 3$ case. The indicated numbers between the two double Sr–O layers in Fig. 1(a) are compatible with the number of n. Figure 1(b) shows a selected-area diffraction pattern taken from a region in Fig. 1(a), and it is composed of both strong Bragg reflections matching the regularity of the $Sr_3V_2O_7$ matrix phase and faint streaks along the c^* direction, which is due to the stacking irregularity along the c direction associated with the intergrowths of $Sr_4V_3O_{10}$.

Figure 2 is also a selected-area diffraction pattern taken from another grain with a beam incidence of [130], and it shows strong Bragg reflections from the $Sr_3V_2O_7$ phase. However, the pattern contains weak additional reflections which are compatible with the pattern for $Sr_4V_3O_{10}$. It is easily

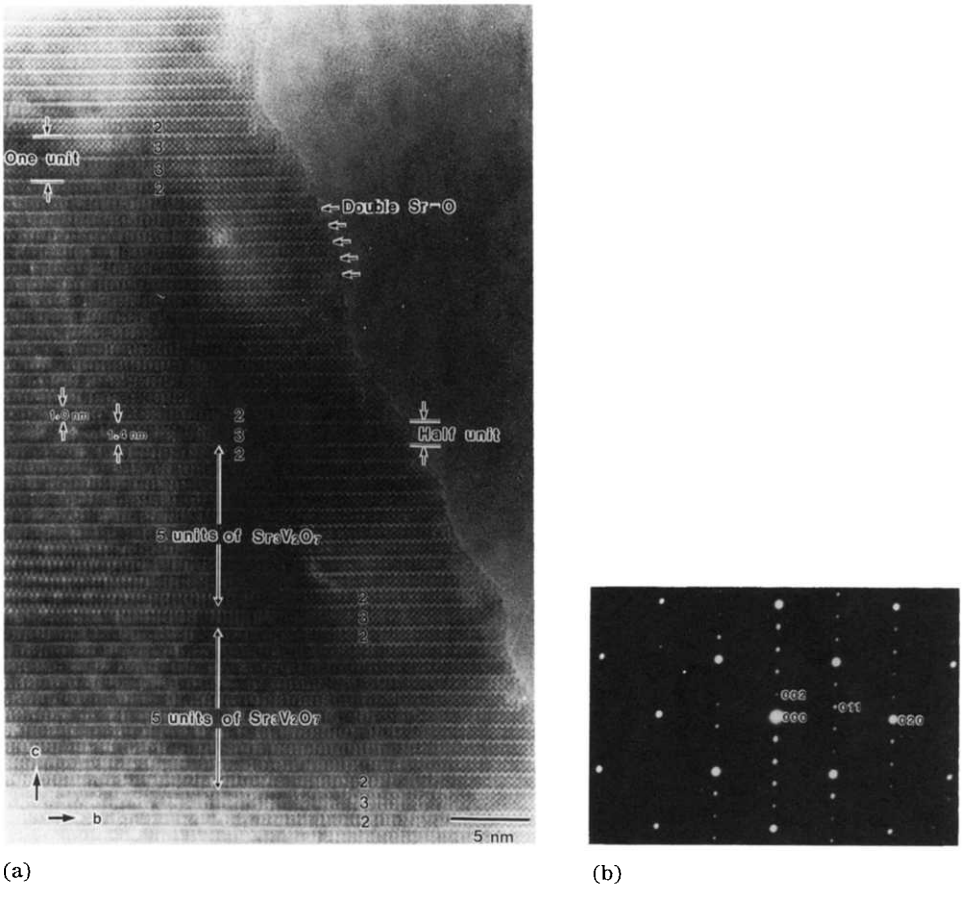

Fig. 1. (a) High resolution image of $Sr_3V_2O_7$ with [100] beam incidence. (b) Selected-area diffraction pattern with [100] incidence.

expected from these results that the intergrowths occur in a wide area for individual grains as seen in the bismuth-based system, and an intergrowth phase which is not the $n=3$ case has not been observed in this study. In previous studies, such intergrowths in a bismuth-based superconducting system have been investigated by Van Tendeloo *et al.* [12], Zandbergen *et al.* [13, 14] and other research groups [15–17]. In the case of the bismuth-based system, the intergrowths often occur between two double Bi–O layers, and different polytypoids are observed in a single grain. In this study, it is elucidated that the two different $Sr_{n+1}V_nO_{3n+1}$ compounds, *i.e.* $n=2$ and $n=3$, are also located in the same grain as seen in the bismuth-based system, and the Sr–O double layer has a structural similarity to the Bi–O double layer in the bismuth-based superconducting system except for the so-called modulated structure. Moreover, it is also remarkable that three types of intergrowth have been observed in the $Sr_3V_2O_7$ matrix. All of them are shown schematically in Figs. 3(ii) (a)–3(ii) (c), which are composed of several types

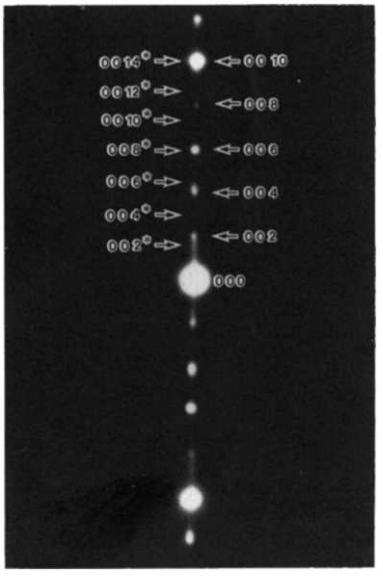

Fig. 2. Selected-area diffraction pattern taken with [130] incidence.

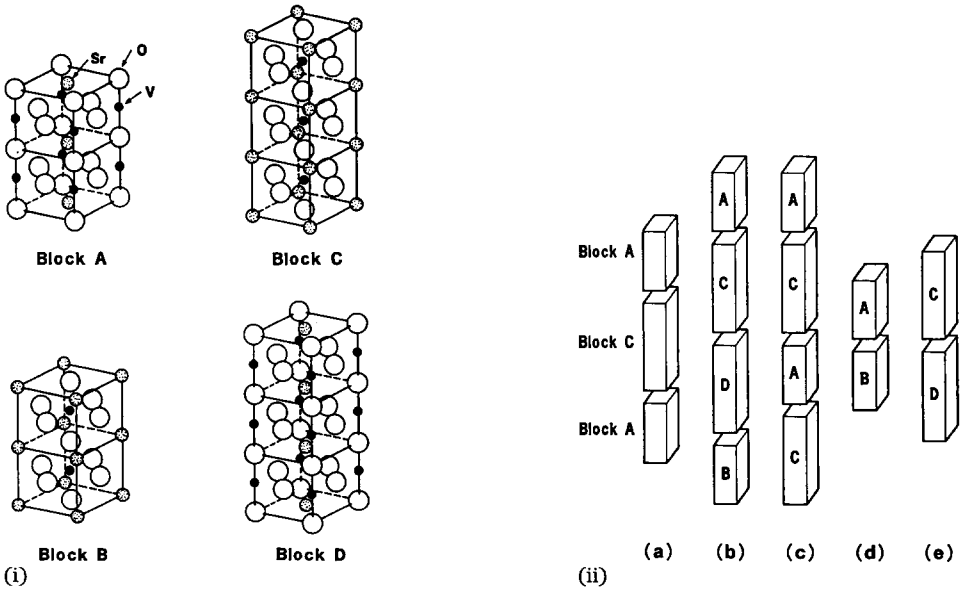

Fig. 3 (i) Schematic representation of four-layered perovskite blocks. (ii) (a)–(c) Possible intergrowth models derived from HREM results, which are composed of the perovskite blocks shown in (i). (d) Unit cell of $Sr_3V_2O_7$. (e) Unit cell of $Sr_4V_3O_{10}$.

of layered perovskite block as shown in Fig. 3(i). Figure 3(ii) (a) shows a half-unit cell of the $Sr_4V_3O_{10}$ growth mode, Fig. 3(ii) (b) shows a one-unit cell of the $Sr_4V_3O_{10}$ growth mode and Fig. 3(ii) (c) shows an alternative

half-unit-cell growth of $Sr_3V_2O_7$ and $Sr_4V_3O_{10}$. The types in Figs. 3(ii) (a), 3(ii) (b) and 3(ii) (c) are composed of stacks of perovskite blocks ACA, ACDB and ACAC respectively. The type in Fig. 3(ii) (a) was the most frequently observed, and the distance between the two intergrowth phases was of the order of 10 nm, *i.e.* about five *c*#unit lengths of $Sr_3V_2O_7$. However, the type in Fig. 3(ii) (c) was not so frequently observed as the types in Figs. 3(ii) (a) and 3(ii) (b). The unit cells of $Sr_3V_2O_7$ and $Sr_4V_3O_{10}$ are also shown schematically in Figs. 3(ii) (d) and 3(ii) (e) respectively. We consider that other types of intergrowth may occur, *e.g.* one-and-a-half-unit-cell growth, two-unit-cell growth, two-and-a-half-unit-cell growth, three-unit-cell growth and so on. Ruddlesden and Popper [19] gave the crystal structure of $Sr_3Ti_2O_7$

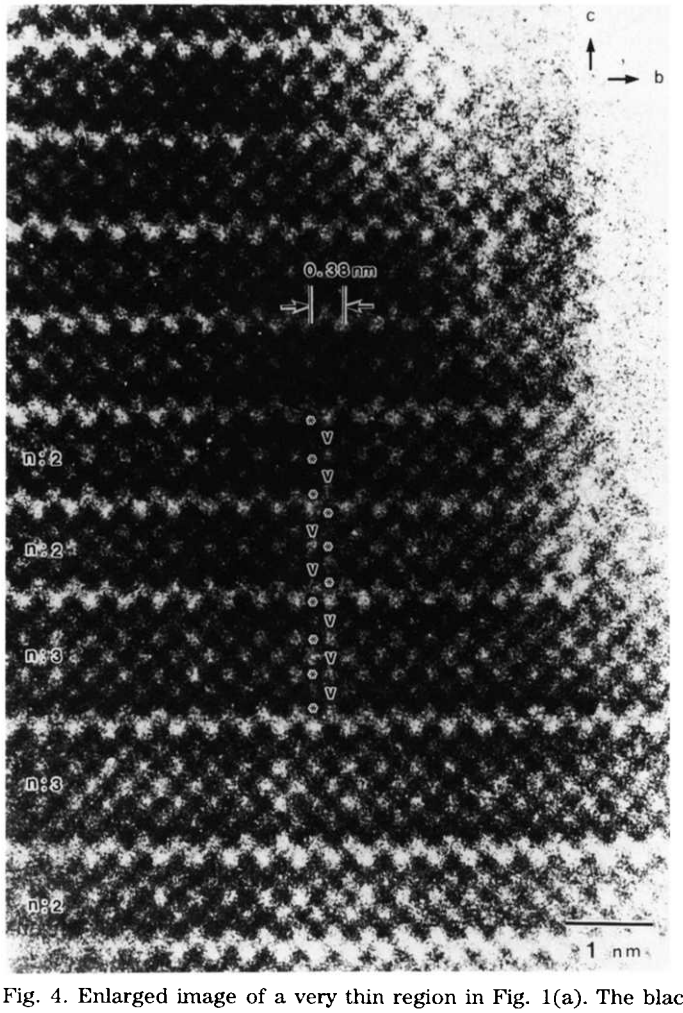

Fig. 4. Enlarged image of a very thin region in Fig. 1(a). The black dots are compatible with projected cationic arrangements. * and V indicate the positions of strontium atoms and vanadium atoms respectively. Coherent $Sr_4V_3O_{10}$ intergrowth ($n=3$) in $Sr_3V_2O_7$ ($n=2$) is clearly visible.

and it is considered that $Sr_3V_2O_7$ is a vanadium-substituted compound for $Sr_3Ti_2O_7$, and the difference between the lattice parameters of these two compounds is very small. The unit cell of $Sr_3V_2O_7$ is expected to be constructed by stacking two types of double perovskite subcell *i.e.* block A and block B, as shown in Fig. 3(ii) (d) [6]. The structural difference between block A and block B is their atomic occupation. However, the volumes of these two subcells are almost equivalent. So, the stacking along the *c* direction of $Sr_3V_2O_7$ can be denoted as ABABABAB. Therefore the interface between block A and block B produces double Sr–O layers about every 1.0 nm. In other words, the crystal lattices on both sides of the interfaces are mutually displaced by a translation vector of $(a/2)$ [110]. We successfully observed such an interfacial structure, as shown in Fig. 4. Figure 4 is a partly enlarged image of Fig. 1(a), and zigzag interfacial images of strontium atomic strings along the *b* direction are clearly visible. On the contrary, many researchers have shown that this kind of atomic shift occurs in the middle of the double Bi–O planes in the bismuth-based superconducting system, and in the middle of the double Tl–O planes in the thallium-based superconducting system [10, 20]. Therefore the $Sr_3V_2O_7$ compound has a structural similarity to the bismuth-based (or thallium-based) superconductors from the viewpoint of such an atomic shift. It is also noteworthy that the atomic arrangement of the interfaces between the $Sr_3V_2O_7$ and $Sr_4V_3O_{10}$ phases are visible as black (or white) zigzag strings along the *b* direction, as shown in Fig. 4, and they are almost the same images as shown in the interface between blocks A and B of the matrix phase. So, the $Sr_4V_3O_{10}$ phase grows epitaxially on the (001) planes of the $Sr_3V_2O_7$ matrix phase, since their *a* and *b* lattice parameters are very close. We consider that such stacking defects are influenced by the matrix composition, and compositional fluctuations often appear on the scale of half a unit cell in the $Sr_3V_2O_7$ compound.

4. Conclusions

We have investigated the local irregular structures in the $Sr_3V_2O_7$ crystal associated with an introduction of the newly discovered intergrowths of $Sr_4V_3O_{10}$. Both the matrix and the intergrowths phases are $Sr_{n+1}V_nO_{3n+1}$ compounds. Three types of intergrowth have been elucidated in the present study, and their structural models have been proposed. The intergrowths are considered to be due to compositional fluctuations. It has been revealed that there is a structural similarity of the defect in atomic stacking to that in the bismuth-based superconducting system.

Acknowledgments

The authors are grateful to M. Azuma, I. Watanabe and H. Yamaguchi for their continuous encouragement.

References

1 J. G. Bednorz and K. A. Muller, *Z. Phys. B, 64* (1986) 189.
2 M. K. Wu, J. R. Ashburn, C. J. Torng, P. H. Hor, R. L. Meng, L. Gao, Z. J. Huang, Y. Q. Wang and C. W. Chu, *Phys. Rev. Lett., 58* (1987) 908.
3 H. Maeda, Y. Tanaka, M. Fukutomi and T. Asano, *Jpn. J. Appl. Phys., 27* (1988) L209.
4 Z. Z. Sheng and A. M. Hermann, *Nature, 332* (1988) 138.
5 M. Cyrot, B. Lambert-Andron, J. L. Soubeyroux, M. J. Rey, PH. Dehauht, F. Cyrot-Lackmann, G. Fourcaudot, J. Beille and J. L. Tholence, *J. Solid State Chem., 85* (1990) 321.
6 A. Nozaki, H. Yoshikawa, T. Wada, H. Yamauchi and S. Tanaka, *Phys. Rev. B, 43* (1991) 181.
7 N. Suzuki, T. Noritake, N. Yamamoto and T. Hioki, *Mater. Res. Bull., 26* (1991) 1.
8 S. Takeno, S. Nakamura, T. Nomaki, N. Fukushima and K. Ando, *J. Solid State Chem., 94* (1991) 432.
9 K. Hiraga, M. Hirabayashi, M. Kikuchi and Y. Syono, *Jpn. J. Appl. Phys., 27* (1988) L573.
10 Y. Matsui, S. Takekawa, H. Nozaki, A. Umezono, E. Takayama-Muromachi and S. Horiuchi, *Jpn. J. Appl. Phys., 27* (1988) L1241.
11 N. Fukushima, S. Tanaka, H. Niu and K. Ando, *Jpn. J. Appl. Phys., 29* (1990) L2190.
12 G. Van Tendeloo, H. W. Zandbergen, J. Van Landuyt and S. Amelinckx, *Appl. Phys. A, 46* (1988) 153.
13 H. W. Zandbergen, Y. K. Huang, M. J. V. Menken, J. N. Li, K. Kodowaki, A. A. Menovsky, G. Van Tendeloo and S. Amelinckx, *Nature, 332* (1988) 620.
14 H. W. Zandbergen, P. Groen, G. Van Tendeloo, J. Van Landuyt, and S. Amelinckx *Solid State Commun., 66* (1988) 397.
15 S. Ikeda, H. Ichinose, T. Kimura, T. Matsumoto, H. Maeda, Y. Ishida and K. Ogawa, *Jpn. J. Appl. Phys., 27* (1988) L999.
16 K. Hiraga, T. Oku, D. Shindo and M. Hirabayashi, *J. Electron Microsc. Tech., 12* (1989) 228.
17 R. Ramesh, B. G. Bagley, J. M. Tarascon, S. M. Green, M. L. Rudee and H. L. Luo, *J. Appl. Phys., 67* (1990) 379.
18 J. M. Cowley and S. Iijima, *Z. Naturforsch., 27a* (1972) 445.
19 S. N. Ruddlesden and P. Popper, *Acta Cryst. Allogr., 11* (1958) 54.
20 M. A. Subramanian, J. C. Calabrese, C. C. Torardi, J. Gopalakrishnan, T. R. Askew, R. B. Flippen, K. J. Morrissey, U. Chowdhry and A. W. Sleiht, *Nature, 332* (1988) 420.